Journal of Computational Science 67 (2023) 101943

Contents lists available at ScienceDirect

Journal of Computational Science

journal homepage: www.elsevier.com/locate/jocs

Multiple classification of EEG signals and epileptic seizure diagnosis with combined deep learning

Muhammet Varlı [a], Hakan Yılmaz [b,*]

[a] The Institute of Graduate Studies, Department of Biomedical Engineering, University of Karabuk, Karabuk, 78050, Turkey
[b] Department of Medical Engineering, University of Karabuk, Karabuk 78050, Turkey

ARTICLE INFO

Keywords:
Epilepsy
Convolutional Neural Network
Recurrent Neural Network
Combined deep learning
Epileptic seizure diagnosis

ABSTRACT

Epilepsy stands out as one of the common neurological diseases. The neural activity of the brain is observed using electroencephalography (EEG), which allows the diagnosis of epilepsy disease. The aim of this study is to create a combined deep learning model that automatically detects epileptic seizure activity, detection of the epileptic region and classifies EEG signals by using images representing the time-frequency components of the time series EEG signal and numerical values of the raw EEG signals. In the study, 3 different public datasets, CHB-MIT, Bern-Barcelona and Bonn EEG records were used. This study presents a combined model using the time sequence of EEG signals and time-frequency-image transformations of time-dependent EEG signals. CWT and STFT methods were used to convert signals to images. Two models were created separately with the images created by CWT and STFT methods. In the Bonn dataset average accuracy rates of 99.07 %, 99.28 %, respectively, in binary classifications and 97.60 % and 98.56 %, respectively, in multiple classifications were obtained with scalogram and spectrogram images. In the Bern-Barcelona and CHB-MIT datasets, 95.46 % and 96.23 % accuracy rates were obtained, respectively. The data combinations brought together in 3 different combinations with the Bonn dataset were underwent to 8-fold cross validation and average accuracy rates of 99.21 % (± 0.56), 99.50 % (± 0.45), and 98.84 % (± 1.58) were obtained. The model we created can detect whether there is epileptic seizure activity in EEG data, detection of the epileptic region and classify EEG signals with a high success rate.

1. Introduction

Epilepsy affects more than 70 million people worldwide [1]. Since it affects so many people, it is known as a neurological disease that many people suffer from worldwide. Epilepsy is a chronic disorder that can occur because of abnormal electrical discharges in nerve cells apart from the brain's regular electrical activity [2]. EEG is considered a non-invasive clinical diagnostic method used to observe the electrical activity of the brain. EEG signals have high time resolution instead of low spatial resolution, which provides an important advantage for signal analysis [3]. It is possible to detect many neurological disorders such as epilepsy, autism, Parkinson's from EEG signals. There are many studies on automatic diagnosis of neurological disorders [4–7]. Studies for epilepsy with EEG signals are generally based on two different approaches, which are machine learning and deep learning. Although both techniques are frequently used today, the number of studies with deep learning has increased rapidly in recent years. A schematic representation of the comparison of machine learning and deep learning approaches is given in Fig. 1.

Signal transformations such as FFT (Fast Fourier Transform), STFT (Short-Time Fourier Transform), and WT (Wavelet Transform) are performed to observe and analyze the behavior of EEG signals in the frequency domain and to reach the characteristics of the signals in the frequency domain. Various statistical parameters are calculated with the features resulting from these transformations. Examples of statistical parameters used in creating the feature vectors of the signal are the average of the absolute values of the coefficients, the maximum, and minimum of the absolute values of the coefficients, standard deviation, variance, and skewness [8]. In the machine learning approach, the features used in the model are selected manually. It aims to use some features obtained from the signals through various statistical calculations. For this reason, many problems can occur in machine learning approaches, such as the occurrence of human-induced errors, the loss of some critical features in the signals by not considering, and the ineffectiveness of large-scale data due to the need for human resources in the process of feature selection.

* Corresponding author.
E-mail address: hakanyilmaz42@gmail.com (H. Yılmaz).

https://doi.org/10.1016/j.jocs.2023.101943
Received 26 July 2022; Received in revised form 24 November 2022; Accepted 3 January 2023
Available online 13 January 2023
1877-7503/

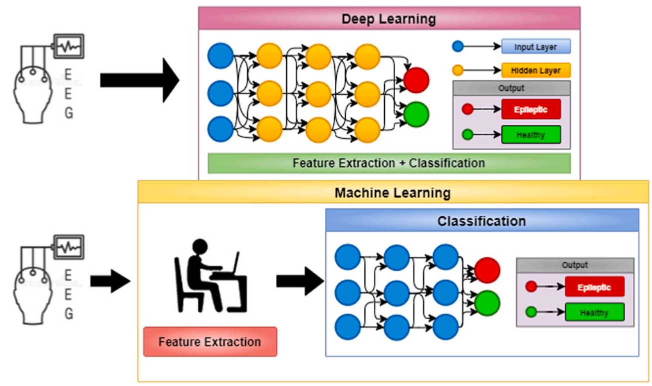

Fig. 1. Comparison of machine learning and deep learning approaches.

In the literature, there are many studies on machine learning approaches conducted with the datasets used in this study. Wang et al. (2017) classified their work based on the combination of non-linear analysis of signals with various classifiers. They obtained an average accuracy rate of 99.25 % with the method they proposed in their study [9]. Mohammadpoory et al. (2017) extracted features from EEG signals with the WVGE (Weighted Visibility Graph Entropy) method and classified the EEG signals with SVM (Support Vector Machine), KNN (K-Nearest Neighbor), DT (Decision Tree), and NB (Naive Bayes) classifiers. As a result of their studies, they classified the EEG signals with an accuracy of 97 % [10]. Akan et al. (2018) separated the EEG signals into IMFs (Intrinsic Mode Functions) with the EMD (Empirical Mode Decomposition) method to perform the time-frequency analysis. Feature vectors were created with Tsallis Entropy, Rényi Entropy, Relative Entropy, and Coherence methods. They classified EEG signals with KNN, LDA (Linear Discriminant Analysis), and NB classification algorithms and obtained 96.97% accuracy value in their study [11]. Rao et al. (2019) used a Random Forest classifier in their research and achieved a success rate of 94.1 % [12]. Sheoran et al. (2020) obtained scalogram images of EEG signals with CWT (Continuous Wavelet Transform). Their study obtained an accuracy value of 99.08 % with the SVM classifier [13]. Akbari and Sadiq (2021), obtained various nonlinear features from EEG signals with EWT (Empirical Wavelet Transform). Then, they applied the KW (Kruskal-Wallis) statistical test to find the important ones among the obtained features. Finally, using the important features obtained from the KW test, they classified the EEG signals with SVM and KNN classifier [14]. Aayesha et al. (2021) performed various preprocessing (signal filtering, signal splitting) on EEG data in Bonn and CHB-MIT dataset. After preprocessing, various temporal and spectral features were extracted by DWT (Discrete Wavelet Transform) method. Then, using these features, they classified the EEG signals with 5 traditional machine learning algorithms, MLP (Multi Layer Perceptron) and 5 fuzzy machine learning algorithms. They obtained the highest results with FRNN (Fuzzy Rough Nearest Neighbor) among the classification algorithms they used [15]. Al-Salman et al. (2022) obtained a set of signal properties using DT CWT (Dual-Tree Complex Wavelet Transform) and FFT methods. Then, using these signal properties, they classified the EEG signals in the Bonn and Bern-Barcelona dataset with the LS-SVM (Least Square Support Vector Machine) classifier [16]. Humairani et al. (2022) filtered the EEG signals of the CHB-MIT dataset with a band-pass filter. Then, they simplified the number of channels with the average channel selection. After decomposing the signals into subbands with DWT, they extracted features from the signals using ShEN (Shannon Entropy) and RE (Renyi's Entropy). Finally, they classified the EEG signals with the SVM algorithm [17].

Deep learning approaches have come to the fore as structures whose use has increased rapidly in recent years. As mentioned earlier, feature extraction is done manually in machine learning approaches. Manual feature extraction can sometimes lead to the loss of important features in complex data not being considered in the classification process. In particular, the fact that the data contains noise and artifacts makes manual feature extraction much more complicated. Manual feature extraction in large-scale data is very time-consuming. In addition, manual feature extraction can cause errors due to the human factor involved in the work. To overcome all these problems, deep learning approaches can be preferred. In the deep learning approach, the features to be used in the model are automatically selected and determined. Deep learning approaches try to learn high-level features in data. The performance of deep learning approaches increases as the data size increases. Deep learning approaches work with multilayer artificial neural networks that mimic the work of nerve cells in the human brain. There is a neuron information transmission system in deep learning structures like humans. The activation function is applied to the data coming to the neurons. Some structures decide which information will reach the output layer according to the result of the function. The high achievements of deep learning structures in recent years and the difficulty of revealing the hidden features in signals with machine learning approaches have played a role in creating this study with deep learning techniques.

In the literature, many studies have been carried out with deep learning approaches using the datasets used in this study. Acharya et al. (2018) classified EEG signals as normal (healthy), seizure-free (inter-ictal), and during seizure (ictal) using the 1D CNN (Convolutional Neural Networks) deep learning structure [18]. Abbasi et al. (2019) first divided the EEG signals into subbands in two equal frequency ranges with DCT (Discrete Cosine Transform). Then, after the Hurst Exponent and ARMA (Autoregressive Moving Average) features were extracted, they were classified with a double-layered LSTM (Long Short-Term Memory) deep learning network. In their study, they classified EEG signals as triple class (healthy, inter-ictal, and ictal) and binary class (inter-ictal and ictal) [19]. Türk and Özerdem (2019) obtained scalogram images by converting EEG signals in the time domain to the frequency domain with the CWT method. Using scalogram images, they classified the EEG recordings in sets A, B, C, D, E in various combinations with a 2D CNN deep learning network [20]. Zhao et al. (2020) classified EEG signals using the 1D CNN deep learning structure [21]. Khan et al. (2021) obtained the EEG signal as multiple single components varying in amplitude and frequency using HVD (Hilbert Vibration Decomposition). After extracting the signal features with HVD, the features selected by correlation-based Q-score were classified using an LSTM-based deep learning model. They conducted their studies with two different datasets, namely Bonn dataset and Sensor Networks Research Lab data [22]. Wang et al. (2021) manually extracted features from EEG signals using EMD and DWT methods used in non-linear feature analysis and automatically using 1D CNN deep learning from 1D signal. With the classical approach, they extracted the time-frequency domain signal wave features to generate a time series feature set from the signal. They abstracted this generated time series feature set through the bidirectional Bi-LSTM-AM (Long Short-Term Memory Attention Machine) classifier. Later, they combined the abstracted classical features with 1D CNN and automatically extracted features. Finally, the classification process was carried out with the MLP classifier. They used the Bonn and Bern-Barcelona datasets, which are also used in this study, to classify the EEG signals [23]. Rashed-Al-Mahfuz et al. (2021) obtained spectrogram images with STFT and scalogram images with CWT by transforming EEG signals from time domain to frequency domain with STFT and CWT methods. Then, they classified the EEG signals by applying multiple models as 4-layer CNN, TL (Transfer Learning) -VGG16, TL-ResNet50, FT (Fine Tuning) -VGG16, and FT-ResNet50 [24]. Ryu and Joe (2021) created a hybrid deep learning model that combines Dense Convolutional Network (DenseNet) and then LSTM for epileptic seizure prediction with CHB-MIT EEG dataset. They used DWT, one of the signal transformation methods, in their studies [25]. Sui et al. (2021) build EEG classification method,a deep learning model called Time-Frequency Hybrid Network (TF-HybridNet). In the created model, STFT and 1d convolution layers are placed in parallel on the EEG data input [26]. Sairamya et al. (2021) first extracted histogram features from EEG signals with QBP (Quad Binary Pattern). Then, the sample entropy, log energy entropy, fuzzy entropy, permutation entropy and approximate entropy were calculated and combined with the QBP features. Finally, EEG recordings are decomposed into subbands using WPD (Wavelet Packet Decomposition) and features are extracted from subbands with QBP. Using all the calculated features, they have classified the focal and unfocal EEG signals with ANN (Artificial Neural Network) [27]. Alharthi et al. (2022) selected various channels from the CHB-MIT dataset and used DWT to decompose the signals. Then, they classified the signals through 1D-CNN, Bi-LSTM and attention deep learning model [28]. Jia et al. (2022) proposed the GCN (Graphical Convolutional Networks) model architecture as a different approach to predict epileptic seizures. Their proposed model includes graph convolution layers, pooling layers and fully connected layers [29]. Gao et al. (2022) split the EEG processing pipeline into two stages, the temporal multiscale stage and the spatial multiscale stage. At each stage in their model, they applied multiscale features along the corresponding dimension and an dilated convolution block on these features [30]. Zhao et al. (2022) used filtering, entropy and STFT to extract features from EEG signals. Three types of supervised learning methods, namely SVM, FCNN (Fully Connected Neural Network) and CNN, were used for classification with the generated signal features. In addition, as a different approach, an acceptable result was obtained by using 15.87% of the EEG data with annotation with PU (Positive Unlabeled) learning [31].

This study aims to provide automatic diagnosis such as the presence of epileptic seizure activity, the separation of epileptic patients and healthy individuals, the separation of epileptic seizures and pre-seizures, the detection of seizure status of epilepsy patients, detection of epilepsy region (focal or non-focal) and multiple classification of EEG signals by using deep learning algorithms. In this study, a combined deep learning model is proposed by merging two different deep learning approaches, CNN (Convolutional Neural Networks) and LSTM (Long-Short Term Memory), which is a type of RNN (Recurrent Neural Networks).

2. Materials and methods

2.1. Datasets

In this study, 3 different public datasets, CHB-MIT, Bern-Barcelona and Bonn, were used for the classification of EEG signals.

2.1.1. CHB-MIT dataset

CHB-MIT Scalp EEG recordings are a fairly large dataset from 22 pediatric samples (5 males, aged 3–22; and 17 females, aged 1.5–19) and one adult patient, grouped in 23 cases. The CHB-MIT dataset contains 916 h of continuous scalp EEG recordings, which are multi-channel and sampled at 256 Hz [32]. In this study, raw EEG recordings from 18 channels (FP1-F7, F7-T7, T7-P7, P7-O1, FP1-F3, F3-C3, C3-P3, P3-O1, FP2-F4, F4-C4, C4-P4, P4-O2, FP2-F8, F8-T8, T8-P8, P8-O2, FZ-CZ, CZ-PZ) were used for epileptic seizure detection without any filtering and preprocessing.

2.1.2. Bern-Barcelona dataset

Bern-Barcelona EEG recordings are a dataset that can be used to detect the pre-surgical epilepsy region. The dataset consists of intracranial EEG recordings from five epilepsy patients. The dataset includes EEG recordings with focal (F) signals from the epileptic region of the brain, and non-focal (NF) signals from the non-epileptic region of the brain [33]. The dataset consists of 3750 focal and 3750 non-focal signal pairs in total. Pair signals represent two adjacent channels (X-Y). All EEG recordings were filtered between 0.5 and 150 Hz with fourth-order Butterworth bandpass filtering. Each EEG recording was recorded with a sampling rate of 1024 for 20 s and then downsampled to 512 Hz. Finally, the median was subtracted for all channels. In this study, the whole dataset, 15,000 EEG signals, was used to classify focal and non-focal EEG recordings. Low pass FIR (Finite Impulse Response) filter was applied for the data used in this study (Passband Frequency: 58 Hz, Stopband Frequency: 65 Hz, Passband Ripple: 1 dB and Stopband Attenuation: 30 Hz).

2.1.3. Bonn dataset

Bonn University dataset contains 5 sets as A–E. Each sequence consists of 100 single-channel EEG signal recordings for a total of 23.6 s [34]. Noises caused by all kinds of muscle movements in EEG recordings have been removed. A, B sets consist of surface EEG recordings (scalp) obtained from 5 healthy patients. Set A was obtained from 5 healthy subjects with their eyes open. Set B was obtained from the same 5 healthy subjects with their eyes closed. C,D (without seizure), E (on seizure) sets consist of intracranial EEG recordings taken from 5 epilepsy patients. Set C is pre-seizure (inter-ictal) from epilepsy patients and includes recordings from the hippocampal hemisphere of the opposite hemispheric region. Set D includes pre-seizure (inter-ictal) recordings of epilepsy patients from the epileptic region. The E set includes the recordings obtained from epilepsy patients while having an epileptic seizure (ictal). EEG recordings are a mixture of scalp (surface) and intracranial recordings. The sampling frequency of EEG data is 173.61 Hz.

2.2. Data pre-processing

In order to increase the number of data in the Bonn dataset, which is smaller than the other datasets used in this study, the data was divided into equal parts. Each EEG record of the Bonn dataset consists of 4097 data points. To segment the dataset into 16 equal parts, the last data points were deleted, and 4096 data points were processed. A total of 1600 observations were generated for each set containing 16 pieces of 256 data points from an EEG recording. Thus, a total of 8000 observations were obtained for 5 sets. The normalization process, the main purpose of which is to prevent the negative effects caused by possible outliers in the dataset, was used only for the data of the Bonn dataset, because the workload is very high due to the large size of the other datasets. In the created model, 1-dimensional EEG signals were used for the RNN part. By switching from the time domain to the frequency domain with EEG signals, the necessary input images for the 2D-CNN structure were obtained. Two different methods, CWT and STFT, were used for the transformations.

2.3. Signal transformations

Signal transformations are performed to provide that EEG signals pass from the time domain to the frequency domain. Signal transformations allow a spectral analysis of signals. Sometimes signals can have important features in the frequency domain, so switching to the frequency domain is necessary. Examples of important signal transformations that allow signals to transition into the frequency domain are FT (Fourier Transform), STFT (Short-Time Fourier Transform), CWT (Continuous Wavelet Transform), DWT (Discrete Wavelet Transform). In this study, STFT and CWT signal transformations were performed to perform frequency analysis of EEG signals. After applying the signal transformations, two-dimensional images of the signals were obtained. Spectrogram images with STFT and scalogram images with CWT are obtained from EEG signals.

2.3.1. Short-Time Fourier Transform

FT is not a suitable method for analyzing non-stationary signals [35]. STFT works by examining only a small part of the signal at a specific time to avoid the problems experienced in FT. Non-stationary signals are divided into small segments, and these segments are considered to be sequential. Thus, FT is applied to each part. These parts are obtained by using a windowing function. This method is called signal windowing.

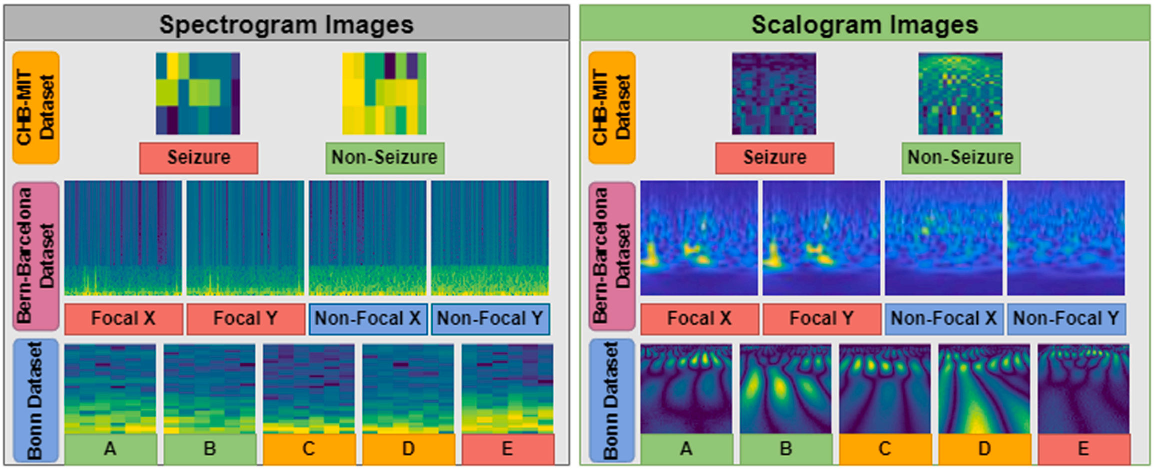

Fig. 2. Spectrogram and scalogram image samples for each dataset.

With STFT, time-dependent signals can be expressed in frequency and time axis. STFT is defined in Eq. (1). Here f(t) represents the signal in the time domain, and W represents the windowing function. Finally, w represents the frequency parameter, t the time parameter, and τ the slow time parameter.

$$\gamma(w,\tau) = STFT\{f(t)\} = \int f(t)W(t-\tau)e^{-jwt}dt \tag{1}$$

In this study, Hamming is used as the windowing function in STFT. For the CHB-MIT, Bern-Barcelona and Bonn datasets, the window sizes were determined as 4,128,64, and the "noverlap" parameter, which is the number of points to overlap between the windows, was determined as 2,64,32, respectively. With STFT, spectrogram images, which are a visual representation of the time-varying spectrum of a signal, were obtained. Each of the generated spectrogram images is 32×32, 64×64, 77×75 for CHB-MIT, Bern-Barcelona and Bonn datasets, respectively. An example of spectrogram images generated with the datasets is shown in Fig. 2.

2.3.2. *Continuous Wavelet Transform*

Wavelet Transform aims to reduce the resolution loss caused by window size selection in STFT [36]. CWT uses a windowing function called the mother wavelet. The difference between this windowing function and the windowing function used in STFT is that it is scalable. While performing CWT, the wavelet function is shifted in time and scaled, as shown in Eq. (2).

$$\psi_{a,b}(t) = \frac{1}{\sqrt{a}}\psi\left(\frac{t-b}{a}\right)a,b \in R, a \neq 0 \tag{2}$$

Here, parameter a represents scaling, and parameter b represents a translation. Low-scale parameters compress the signals while high-scale parameters expand the signals. High-scale parameters capture low frequencies, while low-scale parameters capture high frequencies. The CWT is defined as the integral of the signal to be analyzed with the complex conjugate of the wavelet function, as shown in Eq. (3). Here f(t) represents the time-dependent signal.

$$CWT\{f(t), a, b\} = \int_{-\infty}^{+\infty} f(t)\psi^{*}{}_{a,b}(t)dt \tag{3}$$

Low-frequency information is also considerable for EEG signals. Because the Delta band of EEG signals contains very low frequencies. In this study, the Morlet wavelet function, effective at low frequencies, is used as the mother wavelet function [37]. After performing the CWT transformation, scalogram images of the signal are created according to the coefficients and scale parameters. The scale parameter was determined as 1.5:1.5:90 for the Bern-Barcelona dataset and 1.5:1.5:384 for the CHB-MIT and Bonn datasets. Each of the generated scalogram images is 32×32, 64×64, 77×75 for CHB-MIT, Bern-Barcelona and Bonn datasets, respectively. An example of scalogram images generated with the datasets is shown in Fig. 2.

2.4. *Convolutional Neural Networks*

CNN is a deep learning network that can be used on single, two, or three-dimensional data. CNN was generally created in two-dimensional data, especially images [38]. CNN structures contain various layers.

Convolution Layer: This layer enables the detection of features in the image. It contains low or high-order features in image data. A sample matrix called a filter or kernel is applied to the image to detect these features. The filter matrix scrolls through the image, starting from the top left corner of the image. As the filter matrix moves through the image, the image and filter matrix values are multiplied according to their indices, and the results are summed. Then, the total result is recorded in an output matrix. This process is continued in the same way throughout the whole image. This process is called Convolution. Convolution is shown in Eq. (4) and Eq. (5). The input image is represented by f and the filter by h.

$$G[m,n] = (f*h)[m,n] \tag{4}$$

$$G[m,n] = \sum_j\sum_k h[j,k]f[m-j,n-k] \tag{5}$$

BN (Batch Normalization) Layer: In deep learning structures, each layer works as the input of the next layer. Before the learning process in one layer is finished, the learning process in another layer does not start. The normalization process standardizes input values. However, intermediate layers cannot benefit from the normalization process performed at the beginning. Therefore, problems such as slower, more unstable training or loss of gradient, that is, learning to take place at a minimum level, may be encountered [39]. BN is used to avoid all these problems.

Activation Layer: This layer can be called the non-linear layer. This layer uses non-linear sigmoid, tanh, ReLU, etc., activation functions. Activation functions determine what action a neuron should apply to the input, creating the output. Eq. (6) shows tanh, Eq. (7) sigmoid, Eq. (8) ReLU and Eq. (9) softmax activation function equation.

$$Tanh(x) = \tanh(x) = \frac{\exp(x)-\exp(-x)}{\exp(+x)+\exp(-x)} \tag{6}$$

$$Sigmoid(x) = \sigma(x) = \frac{1}{1+\exp(-x)} \tag{7}$$

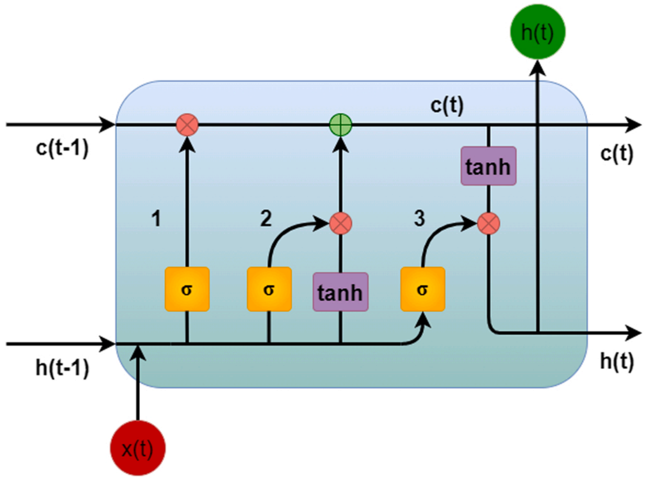

Fig. 3. LSTM block diagram.

$$ReLU(x) = (x)^{+} = \max(0, x) \tag{8}$$

$$S(y)_i = \frac{\exp(y_i)}{\sum_{j=1}^{n} \exp(y_j)} \tag{9}$$

Pooling Layer: The pooling layer works similarly to the convolution layer and reduces the computational load of data by reducing the image size [38]. There are two types of pooling, Max Pooling, and Average Pooling. Max Pooling takes the maximum value of the filter/kernel, navigates, and stores it in the output matrix. Average Pooling takes the average of the part covered by the filter/kernel and stores it in the output matrix. Both pooling methods repeat this process throughout the image, creating the output matrix.

Dropout Layer: This layer allows the neuron units not to be used by inactivating the randomly determined amount during model training. The dropout layer can prevent over-fitting of the model and reduce the workload of the model [40].

Flatten Layer: This layer makes the data into a one-dimensional array. Flatten prepares the input data of the next FC (Full Connected) layer.

FC Layer: Data converted to one-dimensional array shape with

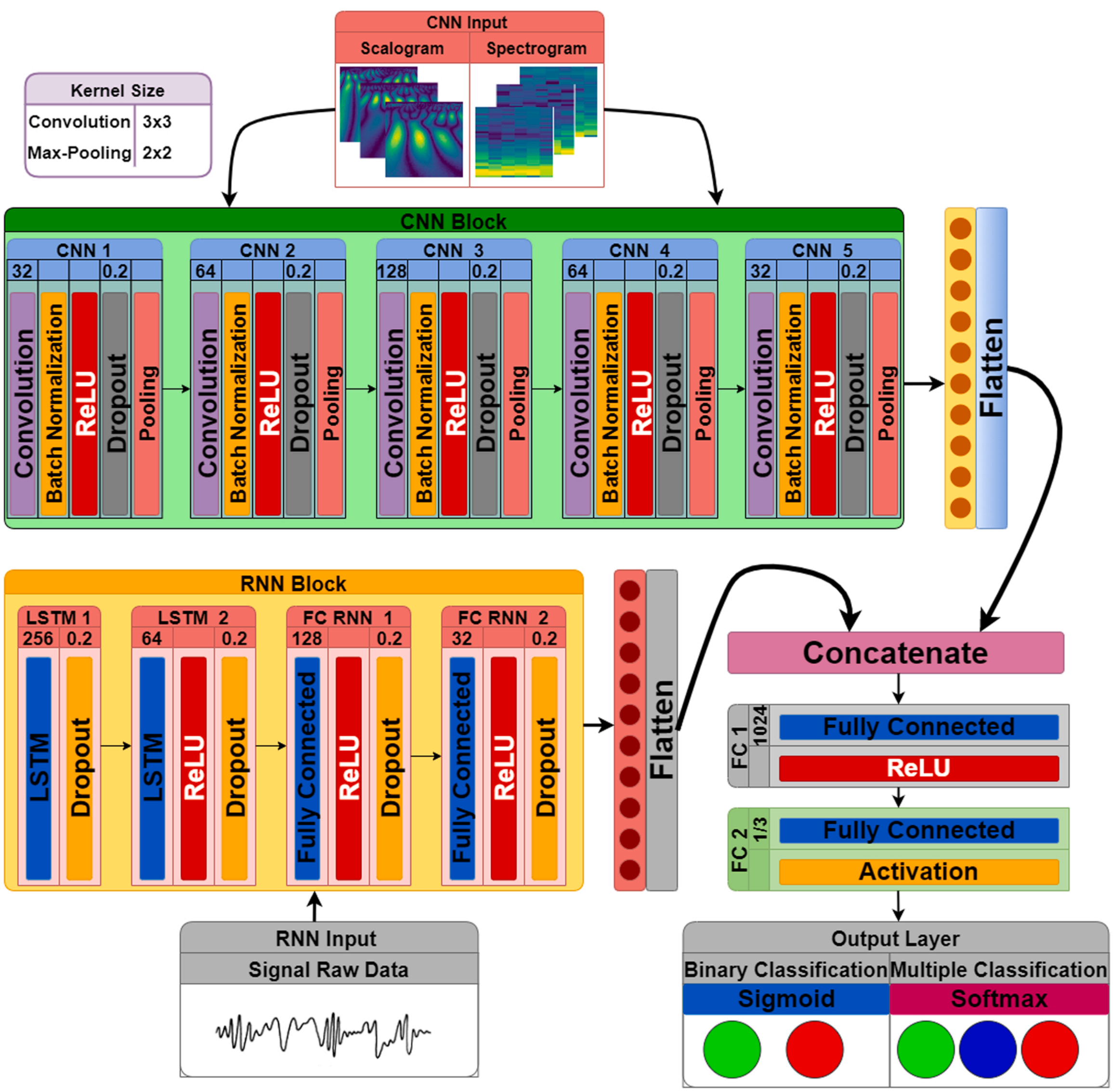

Fig. 4. Model block diagram.

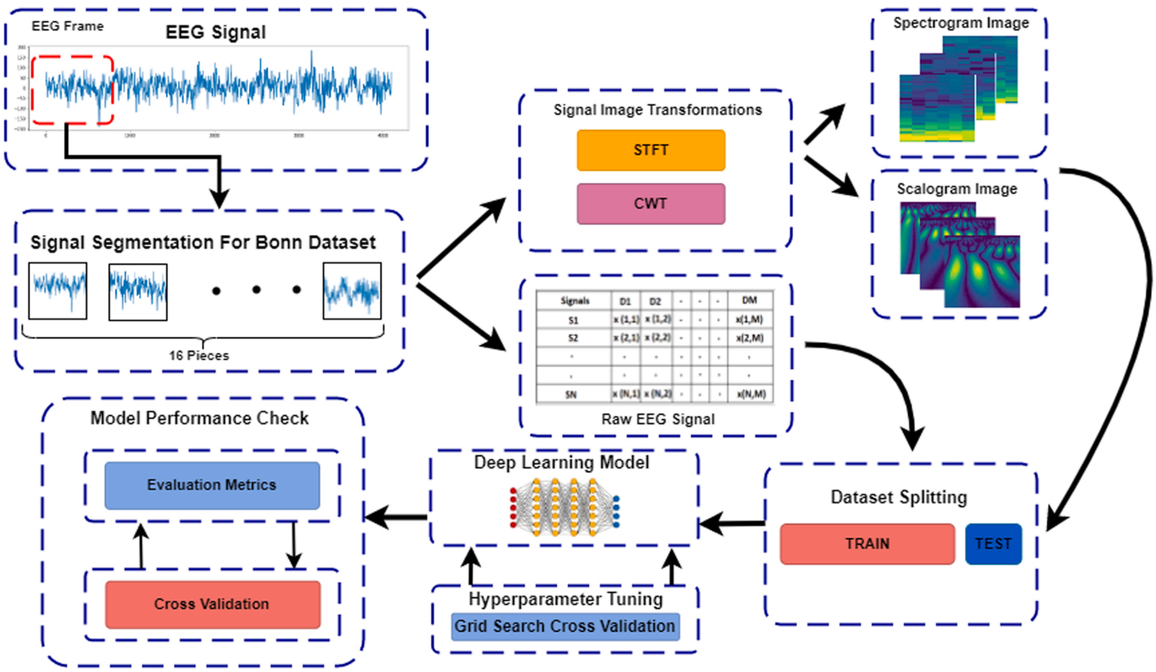

Fig. 5. Summary diagram of the system.

Flatten is the input data of FC. In FC, each input is connected with all neurons.

2.5. Recurrent Neural Networks

RNN is used for time series, natural language processing, and sequential data [39]. Usually, the inputs and outputs in classical deep learning networks are independent. However, in RNNs, the inputs are related to each other. The output from the inputs in the previous layer is stored in memory. So RNNs have a short-term memory. It is used as an input in the other layer. In RNN, each output is dependent on the previous step. The previous inputs affect the output of the next layer. However, this short-term memory of RNN is insufficient in some cases. In addition, the disappearance of gradient in backpropagation may cause learning to remain at a minimum level [39].

LSTM has emerged to prevent these shortcomings of RNN. RNN has one tanh layer. In LSTM, there are four different layers: memory cell, forget gate, input gate, and exit gate [41].

The memory cell is the name given to the transmission line and network memory that carries the important information that should not be forgotten throughout the cells. The short-term memory problem is prevented by this method. The forget gate decides which information to keep in memory and which information to forget through a sigmoid function. The input gate decides whether to update the memory cell by multiplying the previous and next information by the result of the sigmoid operation and the result of the tanh operation. The output gate is used to determine the next cell's input. Previous information and current input are passed through the sigmoid function. Then, the information existing in the memory cell is passed through the tanh function. These two results are multiplied to decide the input information of the next cell. The components in the internal structure of LSTM are shown in Fig. 3. Here, the sigmoid function is expressed with "σ", multiplication with "x" and addition with "+". Finally, x(t) represents the input data, h (t-1) the previous hidden state, c(t-1) the previous cell state, h(t) the new hidden state, and c(t) the new cell state.

2.6. 2D CNN + RNN combined model

In this study, a combined system was created using both CNN and RNN structures. Five layers of CNN are used in the CNN block. A 2-layer of LSTM structure is used in the RNN block. Then both blocks were flattened and merged. After merging, the FC layer is added to the model as if it were a single structure. Then the output layer for the classification layer is added. Since both binary and multiple classification processes are performed in the model, the activation function and number of outputs differ in the output layer. The model output was obtained with the sigmoid activation function for binary classification. The model output was obtained with the softmax activation function for multiple classification. The same model and the same model parameters were used for each dataset used in the study. The model block diagram is shown in Fig. 4.

There are many hyperparameters for the model. These hyperparameters greatly affect the performance of the model. Determining the hyperparameters that give the best performance in the model is a very long process. In model training, the average completion time of 1 epoch is 23, 56, 465 s for Bonn, Bern-Barcelona and CHB-MIT datasets, respectively. However, it is unclear how many epochs the model will be trained. Because some models are stopped if there are an over-fitting or under-fitting situation thanks to the early stop function. The model hyperparameter optimization process was performed with the Bonn dataset due to the large size of the other datasets. On average, the trial process of 10 hyperparameters takes approximately 4–5 h. 32-64-128-64-32, 16-32-64-32-16, and 64-128-256-128-64 were tried for the number of neurons used in the CNN block of the model. In the RNN block, the neuron numbers 256-64-128-32 and 512-128-256-64 were tested. Finally, after combining both blocks, 1024, 512, and 256 neuron numbers were tried as the number of neurons in the FC layer. For CNN block "relu", "tanh", "selu", "elu", "sigmoid" activation functions and for the RNN block ("relu", "sigmoid", "relu"), ("sigmoid", "relu", "relu"), ("relu", "elu", "relu"), ("relu", "relu", "relu") combinations were tried. For the activation function of the FC layer after combining both blocks, "relu" and "elu" functions are tried. "Adam", "Nadam", "SGD", "RMSprop", "Adamax" optimizer types have been tried for optimizer. In the model, the values of 0.1, 0.2, 0.3, 0.4, 0.5, 0.6, 0.7 were tested for the dropout ratio. The values of 4, 8, 16 for batch size have been tried. The upper limit of the learning rate is determined to be 10^{-5}. During the training, the learning rate was changed by the function according to the training process so that the learning continued in the best way. The

Table 1
Binary classification results with scalogram images.

Study	Datasets	Accuracy (%)	Sensitivity (%)	Specificity (%)	f- Score (%)	Precision (%)	MCC (%)	AUC (%)	Confusion Matrix		
2D CNN CWT + LSTM	Bonn A_E	98.97	98.97	98.97	98.97	98.98	97.95	99.94		**A**	**E**
									A	1598	2
									E	31	1569
2D CNN CWT + LSTM	Bonn B_E	99.62	99.62	99.62	99.62	99.63	99.25	99.99		**B**	**E**
									B	1591	9
									E	3	1597
2D CNN CWT + LSTM	Bonn C_E	99.09	99.09	99.09	99.09	99.11	98.20	99.98		**C**	**E**
									C	1599	1
									E	28	1572
2D CNN CWT + LSTM	Bonn D_E	98.56	98.56	98.56	98.56	98.56	97.12	99.73		**D**	**E**
									D	1577	23
									E	23	1577
2D CNN CWT + LSTM	Bonn AB_E	99.46	99.46	99.26	99.46	99.46	98.78	99.97		**AB**	**E**
									AB	3189	11
									E	15	1585
2D CNN CWT + LSTM	Bonn ABC_E	99.23	99.23	98.33	99.23	99.23	97.95	99.93		**ABC**	**E**
									ABC	4785	15
									E	34	1566
2D CNN CWT + LSTM	Bonn ABD_E	99.36	99.36	98.62	99.36	99.36	98.29	99.94		**ABD**	**E**
									ABD	4787	13
									E	28	1572
2D CNN CWT + LSTM	Bonn AC_E	98.83	98.83	98.26	98.83	98.83	97.37	99.87		**AC**	**E**
									AC	3181	19
									E	37	1563
2D CNN CWT + LSTM	Bonn ACD_E	98.91	98.91	97.22	98.90	98.91	97.07	99.84		**ACD**	**E**
									ACD	4788	12
									E	58	1542
2D CNN CWT + LSTM	Bonn AD_E	99.00	99.00	98.44	99.00	99.00	97.75	99.91		**AD**	**E**
									AD	3186	14
									E	34	1566
2D CNN CWT + LSTM	Bonn BC_E	99.46	99.46	99.17	99.46	99.46	98.78	99.98		**BC**	**E**
									BC	3192	8
									E	18	1582
2D CNN CWT + LSTM	Bonn BCD_E	99.47	99.47	98.74	99.47	99.47	98.58	99.95		**BCD**	**E**
									BCD	4792	8
									E	26	1574
2D CNN CWT + LSTM	Bonn BD_E	99.10	99.10	98.71	99.10	99.10	97.98	99.85		**BD**	**E**
									BD	3184	16
									E	27	1573
2D CNN CWT + LSTM	Bonn ABCD_E	99.42	99.42	98.64	99.42	99.42	98.20	99.95		**ABCD**	**E**
									ABCD	6380	20
									E	26	1574
2D CNN CWT + LSTM	Bonn CD_E	98.92	98.92	98.55	98.92	98.92	97.56	99.90		**CD**	**E**
									CD	3177	23
									E	29	1571
2D CNN CWT + LSTM	Bonn AB_CDE	98.34	98.34	98.29	98.34	98.34	96.54	99.72		**AB**	**CDE**
									AB	3142	58
									CDE	75	4725
2D CNN CWT + LSTM	Bern-Barcelona	95.46	94.19	96.73	95.40	96.65	90.95	97.01		**F**	**NF**
									F	7064	436
									NF	245	7255
2D CNN CWT + LSTM	CHB-MIT	96.23	98.20	94.02	96.48	94.82	92.48	97.49		**S**	**NS**
									S	94768	1735
									NS	5178	81469

maximum number of epochs is determined as 300. Trying all these parameters together for the model means making approximately 75,600 trials. Such a large number of attempts requires a lot of time. For this reason, suitable parameters were determined by testing some parameters with each other. Finally, the parameters of the trials with high results were considered together, and the hyperparameters with the best performance were determined. The hyperparameters giving the best results in the model are specified in Fig. 4. Optimizer "Adam", stride parameter 1, and batch size 4 are used in the model.

2.7. Preview the system

In this study, a combined deep learning model that uses two different deep learning structures together has been studied by using both raw EEG data and signal images obtained with STFT and CWT signal transformations. Hyperparameter tuning has been applied to deep learning models. To test whether the model is successful regardless of the partitioning of the dataset, 8-fold cross-validation was performed. Cross-validation was performed with the Bonn dataset due to the large size of the other datasets. Finally, the success of the model was measured with model performance metrics. In Fig. 5. the general working system of this study is shown in a summary diagram.

3. Experimental results and discussion

3.1. Results

In this study, a combined system was created using the signal images obtained by time-frequency image transformation from EEG signals and the raw data of EEG signals. Two separate models with different inputs

Table 2
Binary classification results with spectrogram images.

Study	Datasets	Accuracy (%)	Sensitivity (%)	Specificity (%)	f- Score (%)	Precision (%)	MCC (%)	AUC (%)	Confusion Matrix		
2D CNN STFT + LSTM	Bonn A_E	99.81	99.81	99.81	99.81	99.81	99.63	99.98		**A**	**E**
									A	1600	0
									E	6	1594
2D CNN STFT + LSTM	Bonn B_E	99.94	99.94	99.94	99.94	99.94	99.88	100.00		**B**	**E**
									B	1598	2
									E	0	1600
2D CNN STFT + LSTM	Bonn C_E	99.62	99.62	99.62	99.62	99.63	99.25	99.99		**C**	**E**
									C	1596	4
									E	8	1592
2D CNN STFT + LSTM	Bonn D_E	98.06	98.06	98.06	98.06	98.11	96.17	99.86		**D**	**E**
									D	1594	6
									E	56	1544
2D CNN STFT + LSTM	Bonn AB_E	99.81	99.81	99.81	99.81	99.81	99.58	100.00		**AB**	**E**
									AB	3194	6
									E	3	1597
2D CNN STFT + LSTM	Bonn ABC_E	99.53	99.53	99.47	99.53	99.53	98.75	99.97		**ABC**	**E**
									ABC	4779	21
									E	9	1591
2D CNN STFT + LSTM	Bonn ABD_E	98.55	98.55	98.97	98.56	98.59	96.21	99.94		**ABD**	**E**
									ABD	4720	80
									E	13	1587
2D CNN STFT + LSTM	Bonn AC_E	99.58	99.58	99.45	99.58	99.58	99.06	99.99		**AC**	**E**
									AC	3191	9
									E	11	1589
2D CNN STFT + LSTM	Bonn ACD_E	98.52	98.52	99.13	98.53	98.58	96.15	99.94		**ACD**	**E**
									ACD	4714	86
									E	9	1591
2D CNN STFT + LSTM	Bonn AD_E	99.38	99.38	99.19	99.37	99.37	98.59	99.97		**AD**	**E**
									AD	3186	14
									E	16	1584
2D CNN STFT + LSTM	Bonn BC_E	99.60	99.60	99.58	99.60	99.60	99.11	99.98		**BC**	**E**
									BC	3188	12
									E	7	1593
2D CNN STFT + LSTM	Bonn BCD_E	98.94	98.94	99.06	98.94	98.96	97.20	99.96		**BCD**	**E**
									BCD	4746	54
									E	14	1586
2D CNN STFT + LSTM	Bonn BD_E	99.15	99.15	98.73	99.14	99.15	98.08	99.95		**BD**	**E**
									BD	3186	14
									E	27	1573
2D CNN STFT + LSTM	Bonn CD_E	99.17	99.17	99.05	99.17	99.17	98.13	99.93		**CD**	**E**
									CD	3177	23
									E	17	1583
2D CNN STFT + LSTM	Bonn AB_CDE	99.45	99.45	99.44	99.45	99.45	98.85	99.96		**AB**	**CDE**
									AB	3181	19
									CDE	25	4775
2D CNN STFT + LSTM	Bonn ABCD_E	99.55	99.55	99.04	99.55	99.55	98.59	99.98		**ABCD**	**E**
									ABCD	6382	18
									E	18	1582
2D CNN STFT + LSTM	Bern-Barcelona	93.77	94.49	93.04	93.81	93.14	87.54	95.15		**F**	**NF**
									F	7087	413
									NF	522	6978
2D CNN STFT + LSTM	CHB-MIT	95.08	96.70	93.28	95.40	94.13	90.16	97.05		**S**	**NS**
									S	93321	3182
									NS	5820	80827

were created using spectrogram and scalogram images. It is crucial to get accepted results in the model by using two different deep learning structures, namely CNN and LSTM. To better analyze the models' performances, the A, B, C, D, and E sets in the Bonn dataset were combined with various combinations as binary and multiple, and used in this way. The proposed models have successfully classified binary and multiple classifications. The success of the proposed models was evaluated with various evaluation scores such as accuracy, sensitivity, specificity, f-score, area under curve (AUC), and Matthews correlation coefficient (MCC). In addition, the confusion matrix for each classification combination is also given to show the classification results clearly. The binary classification results of the model trained with scalogram images and 1-dimensional numerical values of the signals are given in Table 1. (For all datasets). The binary classification results of the model trained with spectrogram images and 1-dimensional numerical values of the signals are shown in Table 2. (For all datasets). The multiple classification results of the model trained with scalogram images and 1-dimensional numerical values of the signals are given in Table 3. The triple classification results of the model trained with spectrogram images and 1-dimensional numerical values of the signals are given in Table 4. Cross-validation was performed to show that the created model could get successful results across the entire dataset. 8-fold cross-validation was performed using the cross validator. Since the sizes of the other datasets used in this study are very large, there is a lot of workload for cross validation, so only the Bonn dataset was cross-validated. To save time due to the high workload, 8-fold cross-validation was performed by choosing the combinations AB_CDE, ABCD_E, and AB_CD_E. The accuracy values obtained for the cross-validations are given in Table 5. Using the Bern-Barcelona dataset, EEG signals were classified as F(Focal) and NF(Non-Focal). For the CHB-MIT dataset, it was classified as S(Seizure)

Table 3
Multiple classification results with scalogram images.

Study	Datasets	Accuracy (%)	Sensitivity (%)	Specificity (%)	f- Score (%)	Precision (%)	MCC (%)	AUC (%)	Confusion Matrix			
2D CNN CWT + LSTM	Bonn A-C-E	96.19	96.19	98.09	96.19	96.23	94.30	99.58		**A**	**C**	**E**
									A	1554	35	11
									C	95	1493	12
									E	13	17	1570
2D CNN CWT + LSTM	Bonn A-D-E	96.65	96.65	98.32	96.65	96.74	95.01	99.69		**A**	**D**	**E**
									A	1586	12	2
									D	46	1545	9
									E	57	35	1508
2D CNN CWT + LSTM	Bonn B-C-E	99.00	99.00	99.50	99.00	99.00	98.50	99.97		**B**	**C**	**E**
									B	1581	14	5
									C	12	1581	7
									E	3	7	1590
2D CNN CWT + LSTM	Bonn B-D-E	98.65	98.65	99.32	98.65	98.65	97.97	99.94		**B**	**D**	**E**
									B	1585	8	7
									D	4	1572	24
									E	3	19	1578
2D CNN CWT + LSTM	Bonn AB-CD-E	97.30	97.30	98.35	97.30	97.31	95.78	99.78		**AB**	**CD**	**E**
									AB	3110	84	6
									CD	62	3116	22
									E	12	30	1558
2D CNN CWT + LSTM	Bonn A-CD-E	96.61	96.61	98.19	96.62	96.67	94.61	99.64		**A**	**CD**	**E**
									A	1548	40	12
									CD	112	3072	16
									E	12	25	1563
2D CNN CWT + LSTM	Bonn B-CD-E	97.98	97.98	98.48	97.98	97.99	96.77	99.78		**B**	**CD**	**E**
									B	1561	33	6
									CD	10	3166	24
									E	8	48	1544
2D CNN CWT + LSTM	Bonn AB-C-E	97.80	97.80	99.02	97.81	97.85	96.51	99.85		**AB**	**C**	**E**
									AB	3107	85	8
									C	21	1570	9
									E	3	15	1582
2D CNN CWT + LSTM	Bonn AB-D-E	98.22	98.22	98.95	98.22	98.22	97.15	99.86		**AB**	**D**	**E**
									AB	3171	26	3
									D	41	1548	11
									E	3	30	1567

and NS(Non-Seizure) according to the presence of seizure activity.

As can be seen from the accuracy rates obtained as a result of cross-validation, both proposed models achieve high accuracy rates regardless of the partitioning of the dataset. These results show that our model works well not only at a certain point of the dataset but also at different points. The expression “std” in Table 5. refers to the standard deviation. The highest accuracy rate obtained for binary classification was 99.94 % with the combination of B_E in the 2D CNN STFT + LSTM model. The highest accuracy rate obtained for the multiple classification was obtained as 99.31 % with the combination of B-C-E in the 2D CNN STFT + LSTM model. The results obtained with both models are very close to each other. In some combinations, the 2D CNN CWT + LSTM model using scalogram images achieved higher results, but in general, the 2D CNN STFT + LSTM model using spectrogram images achieved better results in most dataset combinations.

3.2. Discussion

EEG signals are used to diagnose many neurological diseases, especially epilepsy. Due to the widespread development of machine learning and deep learning approaches, many advances have occurred, such as signal processing, feature extraction from signals, and automatic disease detection. In this study, 2D CNN CWT + LSTM and 2D CNN STFT + LSTM models were carried out for the detection of epilepsy disease, detection of epileptic region in the brain (focal and nonfocal) and multiple classification of EEG signals. As a result of the results obtained, significant clinical success has been achieved. In the 2D CNN CWT + LSTM model, a model using the scalogram images obtained by CWT, one of the signal time-frequency-image transformations, and the one-dimensional numerical values of the signals were created. In the 2D CNN STFT + LSTM model, a model using the one-dimensional numerical values of the signals and the spectrogram images obtained by STFT, one of the signal time-frequency-image transformations, was created. The created model showed successful results in 3 different datasets, showing that it is a method applicable to different EEG data. The fact that it obtains high results without any preprocessing and filtering, especially in a very large dataset such as CHB-MIT, confirms this. There are studies with images of signals using such signal transformations in the literature.

The proposed model uses the CNN structure and uses the LSTM structure, which is a type of RNN. In this respect, it stands out as a combined model. The model achieved better results in many dataset combinations than studies conducted on the same dataset in the literature. For other datasets used in this study, the model gives similar results to the studies in the literature. In addition, multi-class combinations of A-CD-E, B-CD-E, AB-C-E and AB-D-E were used in this study for the Bonn dataset, which are different from other studies in the literature. Through these different multi class combinations, EEG data can be classified by multiple classification as healthy, inter-ictal, and ictal. In addition to the previously existing multi class classification combinations, these classification combinations have been gained in the literature. Since the deep learning approach was used in this study, comparisons were made with other studies using deep learning in the literature. Comparison of binary classification results obtained by similar studies using Bonn, Bern-Barcelona and CHB-MIT datasets with binary classification results in this study is given in Fig. 6, Fig. 7 and Fig. 8., respectively. The comparison of multiclassification results obtained from similar studies using Bonn dataset with the multiclassification results in this study is shown in Fig. 9. In the figures, the proposed method-1 refers to the model using spectrogram images, and the proposed method-2 refers to

Table 4
Multiple classification results with spectrogram images.

Study	Datasets	Accuracy (%)	Sensitivity (%)	Specificity (%)	f- Score (%)	Precision (%)	MCC (%)	AUC (%)	Confusion Matrix			
2D CNN STFT + LSTM	Bonn A-C-E	98.04	98.04	99.02	98.03	98.06	97.08	99.86		**A**	**C**	**E**
									A	1586	11	3
									C	40	1527	33
									E	3	4	1593
2D CNN STFT + LSTM	Bonn A-D-E	99.02	99.02	99.51	99.02	99.02	98.53	99.93		**A**	**D**	**E**
									A	1594	6	0
									D	21	1570	9
									E	1	10	1589
2D CNN STFT + LSTM	Bonn B-C-E	99.31	99.31	99.66	99.31	99.32	98.97	99.98		**B**	**C**	**E**
									B	1591	7	2
									C	3	1593	4
									E	0	7	1583
2D CNN STFT + LSTM	Bonn B-D-E	99.02	99.02	99.51	99.02	99.02	98.53	99.96		**B**	**D**	**E**
									B	1596	4	0
									D	1	1572	27
									E	0	15	1585
2D CNN STFT + LSTM	Bonn AB-CD-E	98.20	98.20	98.99	98.09	98.20	97.19	99.90		**AB**	**CD**	**E**
									AB	3164	34	2
									CD	41	3125	34
									E	0	33	1567
2D CNN STFT + LSTM	Bonn A-CD-E	98.20	98.20	99.09	98.20	98.22	97.14	99.90		**A**	**CD**	**E**
									A	1587	13	0
									CD	55	3116	29
									E	1	17	1582
2D CNN STFT + LSTM	Bonn B-CD-E	98.97	98.97	99.35	98.97	98.97	98.35	99.94		**B**	**CD**	**E**
									B	1592	7	1
									CD	2	3164	34
									E	0	22	1578
2D CNN STFT + LSTM	Bonn AB-C-E	98.22	98.22	99.05	98.21	98.22	97.15	99.90		**AB**	**C**	**E**
									AB	3167	31	2
									C	34	1527	39
									E	0	8	1592
2D CNN STFT + LSTM	Bonn AB-D-E	98.03	98.03	99.21	98.03	98.07	96.87	99.89		**AB**	**D**	**E**
									AB	3161	18	21
									D	12	1529	59
									E	1	15	1584

Table 5
Cross validation accuracy results with various combinations.

Study	Datasets	K1	K2	K3	K4	K5	K6	K7	K8	Mean	Std
2D CNN STFT+ LSTM	Bonn AB_CDE	97.90	99.05	99.00	99.55	99.35	99.30	99.70	99.80	99.21	± 0.56
2D CNN CWT+ LSTM	Bonn AB_CDE	94.50	97.20	97.75	98.55	98.70	99.15	99.50	99.80	98.14	± 1.6
2D CNN STFT+ LSTM	Bonn ABCD_E	97.75	98.75	98.60	99.30	99.45	99.80	99.55	99.85	99.13	± 0.67
2D CNN CWT+ LSTM	Bonn ABCD_E	98.45	99.20	99.55	99.65	99.80	99.75	99.85	99.85	99.50	± 0.45
2D CNN STFT+ LSTM	Bonn AB_CD_E	95.05	97.85	98.95	99.50	99.60	99.95	99.90	99.90	98.84	± 1.58
2D CNN CWT+ LSTM	AB_CD_E	94.40	97.65	98.90	98.65	99.40	99.65	99.90	99.85	98.55	± 1.72

the model using scalogram images. Accuracy, sensitivity, specificity are expressed as Acc, Sen, Spe, respectively. Comparison results are given as a percentage.

4. Conclusion

In this study, a combined deep learning model that automatically detects epileptic seizure activity and classifies EEG signals using the numerical values of raw EEG signals and signal images obtained with two different signal transformations representing the time-frequency components of time series EEG signals has been studied. This study classified the EEG signals of healthy and epileptic subjects with high accuracy, such as healthy-interictal(seizure-free)-ictal(seizure activity) in multiple classification and healthy-epileptic in binary classification. In addition, it can classify EEG signals as focal and non-focal with high accuracy for the detection of epileptic region in the brain. It has been observed that the model created with the Bonn, Bern-Barcelona and CHB-MIT datasets, which are publicly available datasets, has competitive results with other studies in the literature. In the proposed model, two different deep learning structures are used as a combined deep learning structure as a single model. It is observed that the proposed model has higher performance in many of the combinations of the dataset used in similar studies in the literature. The proposed model has also achieved high success in the large datasets CHB-MIT and Bern-Barcelona datasets. Two different signal transformations methods, STFT and CWT, were used in the study. As it can be understood from the results obtained, signal transformations play a significant role in revealing the important properties of biosignals such as EEG by the model. Unlike the studies on the same datasets, the proposed model brings a different perspective to the literature in terms of working with a combined model by using two different deep learning structures together. It stands out as a very successful model in terms of the results it obtained with a combined model using two different deep learning structures. The similar results of the proposed model in both scalogram and spectrogram images reveal the success of the proposed model. As can be seen from the cross-validation results of the proposed model, it confirms that the model performs well not only in one part of the dataset but also in different parts. This study has achieved clinically important

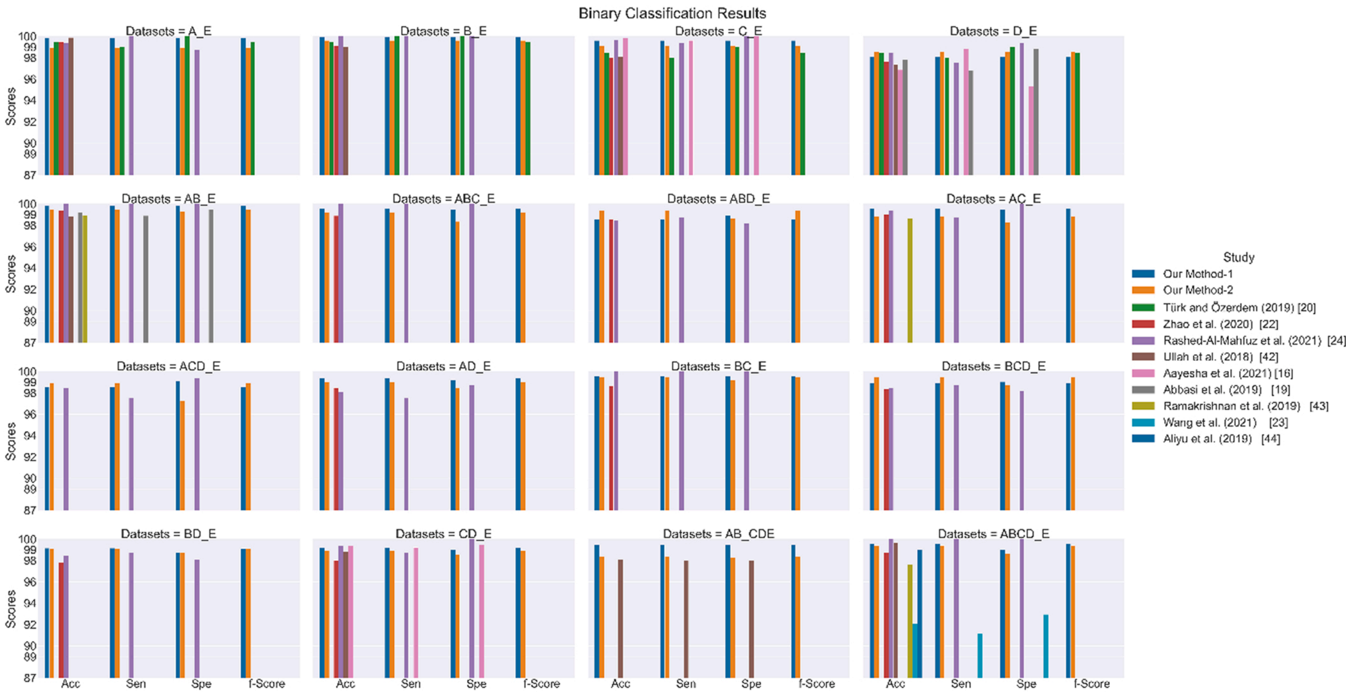

Fig. 6. Comparison with binary classification results obtained in similar studies for Bonn dataset [20, 22, 24, 42, 16, 19, 43, 23, 44].

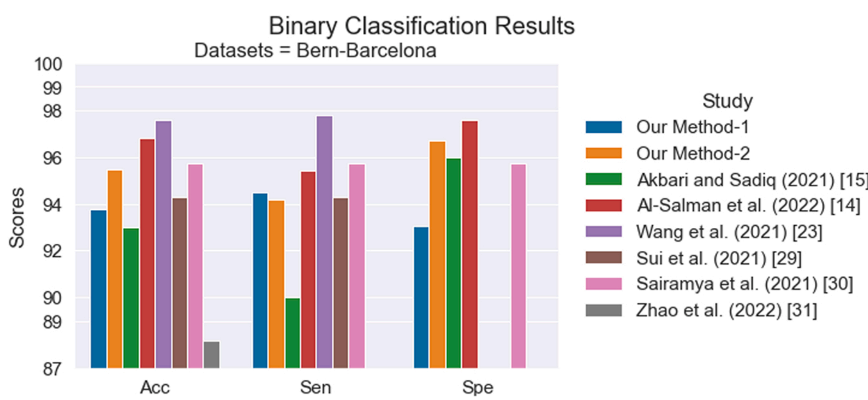

Fig. 7. Comparison with binary classification results obtained in similar studies for Bern-Barcelona dataset [15, 14, 23, 29-31].

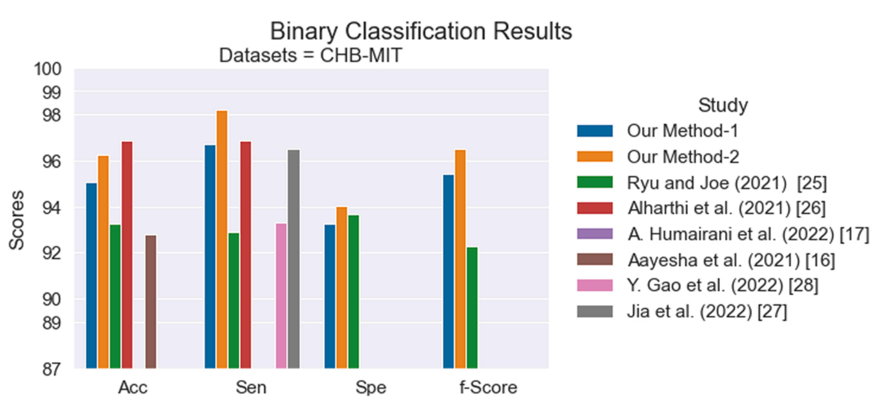

Fig. 8. Comparison with binary classification results obtained in similar studies for CHB-MIT dataset [25, 26, 17, 16, 28, 27].

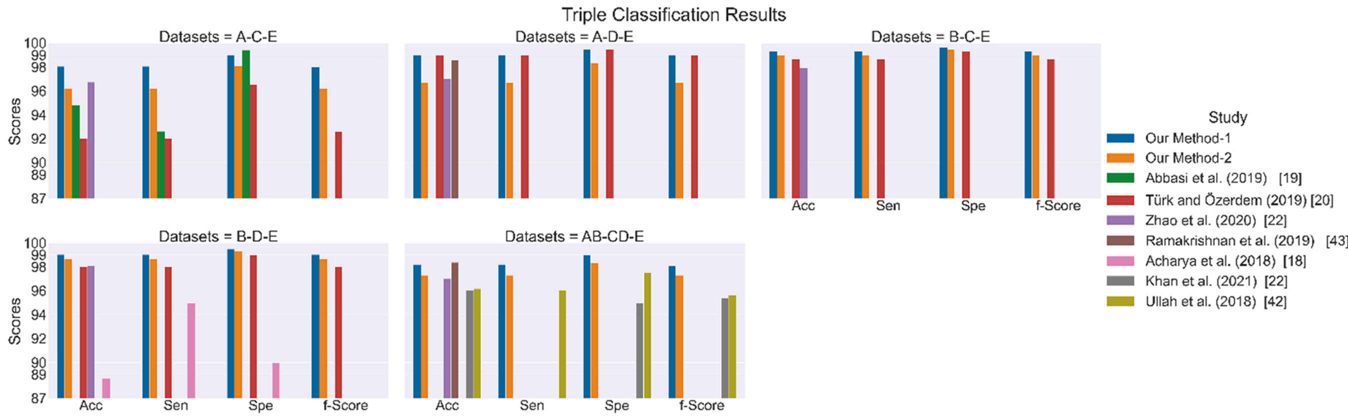

Fig. 9. Comparison with multiple classification results obtained in similar studies for Bonn dataset [19, 20, 22, 43, 18, 22, 42].

results in terms of different approaches it has brought to the literature, its ability to implement with different datasets, its adaptability to different classification scenarios without any change and its high scores.

CRediT authorship contribution statement

All authors have read and approved the manuscript, and all of them have participated in the research process. **Muhammet Varli:** Conceptualization, Methodology, Software, Validation, Writing – original draft, Writing – review & editing, Visualization. **Hakan Yilmaz:** Conceptualization, Methodology, Validation, Writing – review & editing, Supervision.

Declaration of Competing Interest

The authors declare that they have no known competing financial interests or personal relationships that could have appeared to influence the work reported in this paper.

Data Availability

Public datasets were used.

References

[1] A. Singh, S. Trevick, The epidemiology of global epilepsy, Neurol. Clin. 34 (4) (2016) 837–847.
[2] E. Beghi, The epidemiology of epilepsy, Neuroepidemiology 54 (2) (2020) 185–191.
[3] P. van Mierlo, B.J. Vorderwülbecke, W. Staljanssens, M. Seeck, S. Vulliémoz, Ictal EEG source localization in focal epilepsy: review and future perspectives, Clin. Neurophysiol. 131 (11) (2020) 2600–2616.
[4] Brian Penchina, Avirath Sundaresan, Sean Cheong, Victoria Grace, Antoni Valero-Cabré, Adrien Martel, Brain Inform. (2021).
[5] S.A.A. Shah, L. Zhang, A. Bais, Dynamical system based compact deep hybrid network for classification of Parkinson disease related EEG signals, Neural Netw. 130 (2020) 75–84.
[6] J. Sun, R. Cao, M. Zhou, W. Hussain, B. Wang, J. Xue, J. Xiang, A hybrid deep neural network for classification of schizophrenia using EEG data, Sci. Rep. 11 (1) (2021) 4706.
[7] A. Sundaresan, B. Penchina, S. Cheong, V. Grace, A. Valero-Cabré, A. Martel, Evaluating deep learning EEG-based mental stress classification in adolescents with autism for breathing entrainment BCI, Brain Inform. 8 (1) (2021) 13.
[8] L. Hussain, Detecting epileptic seizure with different feature extracting strategies using robust machine learning classification techniques by applying advance parameter optimization approach, Cogn. Neurodyn. 12 (3) (2018) 271–294.
[9] L. Wang, W. Xue, Y. Li, M. Luo, J. Huang, W. Cui, C. Huang, Automatic epileptic seizure detection in EEG signals using multi-domain feature extraction and nonlinear analysis, Entropy 19 (6) (2017).
[10] Z. Mohammadpoory, M. Nasrolahzadeh, J. Haddadnia, Epileptic seizure detection in EEGs signals based on the weighted visibility graph entropy, Seizure 50 (2017) 202–208.
[11] S. Yol, M. Özdemir, A. Akan, L. Chaparro, Detection of Epileptic Seizures by the Analysis of EEG Signals Using Empirical Mode Decomposition, 2018.
[12] M. Ravi Kumar, Y. Srinivasa Rao, Epileptic seizures classification in EEG signal based on semantic features and variational mode decomposition, Cluster Comput., vol. 22 (no. 6), 2019, pp. 13521–31.
[13] P. Sheoran, N. Rathee, J.S. Saini, Epileptic seizure detection using bidimensional empirical mode decomposition and distance metric learning on scalogram, in: Proceedings of the 2020 7th International Conference on Signal Processing and Integrated Networks (SPIN), 2020.
[14] H. Akbari, M.T. Sadiq, Detection of focal and non-focal EEG signals using non-linear features derived from empirical wavelet transform rhythms, Phys. Eng. Sci. Med. 44 (1) (2021) 157–171.
[15] M.B. Aayesha, Qureshi, M. Afzaal, M.S. Qureshi, M. Fayaz, Machine learning-based EEG signals classification model for epileptic seizure detection, Multimed. Tools Appl. 80 (12) (2021) 17849–17877.
[16] W. Al-Salman, Y. Li, P. Wen, F.S. Miften, A.Y. Oudah, H.R.A. Ghayab, Extracting epileptic features in EEGs using a dual-tree complex wavelet transform coupled with a classification algorithm, Brain Res. 147777 (1779) 2022.
[17] A. Humairani, A. Rizal, I. Wijayanto, S. Hadiyoso, Y.N. Fuadah, Wavelet-based entropy analysis on EEG signal for detecting seizures, in: Proceedings of the 2022 10th International Conference on Information and Communication Technology (ICoICT), 2022.
[18] U.R. Acharya, S.L. Oh, Y. Hagiwara, J.H. Tan, H. Adeli, Deep convolutional neural network for the automated detection and diagnosis of seizure using EEG signals, Comput. Biol. Med. 100 (2018) 270–278.
[19] M.U. Abbasi, A. Rashad, A. Basalamah, M. Tariq, Detection of epilepsy seizures in neo-natal EEG using LSTM architecture, IEEE Access 7 (2019) 179074–179085.
[20] Ö. Türk, M.S. Özerdem, Epilepsy detection by using scalogram based convolutional neural network from EEG signals, Brain Sci. 9 (5) (2019) 115.
[21] W. Zhao, W. Zhao, W. Wang, X. Jiang, X. Zhang, Y. Peng, B. Zhang, G. Zhang, A novel deep neural network for robust detection of seizures using EEG signals, Comput. Math. Methods Med. 2020 (2020) 9689821.
[22] P. Khan, Y. Khan, S. Kumar, M.S. Khan, A.H. Gandomi, HVD-LSTM based recognition of epileptic seizures and normal human activity, Comput. Biol. Med. 136 (2021), 104684.
[23] Y. Wang, Y. Dai, Z. Liu, J. Guo, G. Cao, M. Ouyang, D. Liu, Y. Shan, G. Kang, G. Zhao, Computer-aided intracranial EEG signal identification method based on a multi-branch deep learning fusion model and clinical validation, Brain Sci. 11 (5) (2021).
[24] M. Rashed-Al-Mahfuz, M.A. Moni, S. Uddin, S.A. Alyami, M.A. Summers, V. Eapen, A deep convolutional neural network method to detect seizures and characteristic frequencies using epileptic electroencephalogram (EEG) data, IEEE J. Transl. Eng. Health Med. 9 (2021) 1–12.
[25] S. Ryu, I. Joe, A hybrid denseNet-LSTM model for epileptic seizure prediction, Appl. Sci. 11 (16) (2021).
[26] L. Sui, X. Zhao, Q. Zhao, T. Tanaka, J. Cao, Hybrid convolutional neural network for localization of epileptic focus based on iEEG, Neural Plast. 2021 (2021) 6644365.
[27] N.J. Sairamya, M.S.P. Subathra, E.S. Suviseshamuthu, S. Thomas George, A new approach for automatic detection of focal EEG signals using wavelet packet decomposition and quad binary pattern method, Biomed. Signal Process. Control 63 (2021), 102096.
[28] M.K. Alharthi, K.M. Moria, D.M. Alghazzawi, H.O. Tayeb, Epileptic disorder detection of seizures using EEG signals, Sensors 22 (17) (2022).
[29] M. Jia, W. Liu, J. Duan, L. Chen, C. Chen, Q. Wang, Z. Zhou, Efficient graph convolutional networks for seizure prediction using scalp EEG, Front. Neurosci. 16 (2022), 967116.
[30] Y. Gao, X. Chen, A. Liu, D. Liang, L. Wu, R. Qian, H. Xie, Y. Zhang, Pediatric seizure prediction in scalp EEG using a multi-scale neural network with dilated convolutions, IEEE J. Transl. Eng. Health Med. 10 (2022) 1–9.
[31] X. Zhao, Q. Zhao, T. Tanaka, J. Solé-Casals, G. Zhou, T. Mitsuhashi, H. Sugano, N. Yoshida, J. Cao, Classification of the epileptic seizure onset zone based on partial annotation, Cogn. Neurodyn (2022).

[32] A. Shoeb, J. Guttag, Application of machine learning to epileptic seizure detection, in: ICML 2010 - Proceedings, 27th International Conference on Machine Learning, 982 975, 2010.
[33] R. Andrzejak, K. Schindler, C. Rummel, Nonrandomness, nonlinear dependence, and nonstationarity of electroencephalographic recordings from epilepsy patients, Phys. Rev. E Stat. Nonlinear Soft Matter Phys. 86 (2012), 046206.
[34] R.G. Andrzejak, K. Lehnertz, F. Mormann, C. Rieke, P. David, C.E. Elger, Indications of nonlinear deterministic and finite-dimensional structures in time series of brain electrical activity: dependence on recording region and brain state, Phys. Rev. E 64 (6) (2001), 061907.
[35] M.K. Kıymık, İ. Güler, A. Dizibüyük, M. Akın, Comparison of STFT and wavelet transform methods in determining epileptic seizure activity in EEG signals for real-time application, Comput. Biol. Med. 35 (7) (2005) 603–616.
[36] B. Rajoub, Chapter 2 – characterization of biomedical signals: feature engineering and extraction. Biomedical Signal Processing and Artificial Intelligence in Healthcare, Academic Press, 2020, pp. 29–50.
[37] N. Bajaj, Wavelets for EEG Analysis, 2020.
[38] S. Indolia, A.K. Goswami, S.P. Mishra, P. Asopa, Conceptual understanding of convolutional neural network – a deep learning approach, Int. Conf. Comput. Intell. Data Sci. 132 (2018) 679–688.
[39] L. Alzubaidi, J. Zhang, A.J. Humaidi, A. Al-Dujaili, Y. Duan, O. Al-Shamma, J. Santamaría, M.A. Fadhel, M. Al-Amidie, L. Farhan, Review of deep learning: concepts, CNN architectures, challenges, applications, future directions, J. Big Data 8 (1) (2021) 53.
[40] J. Gu, Z. Wang, J. Kuen, L. Ma, A. Shahroudy, B. Shuai, T. Liu, X. Wang, G. Wang, J. Cai, T. Chen, Recent advances in convolutional neural networks, Pattern Recognit. 77 (2018) 354–377.
[41] G. Chen, A Gentle Tutorial of Recurrent Neural Network with Error Backpropagation, 2016.
[42] I. Ullah, M. Hussain, E.-H. Qazi, H. Aboalsamh, An automated system for epilepsy detection using EEG brain signals based on deep learning approach, Expert Syst. Appl. 107 (2018) 61–71.
[43] S. Ramakrishnan, A.S. Muthanantha, Murugavel P. Saravanan, Epileptic EEG signal classification using multi-class convolutional neural network, in: Proceedings of the 2019 International Conference on Vision Towards Emerging Trends in Communication and Networking (ViTECoN), 2019.
[44] I. Aliyu, Y. Lim, C. Lim, Epilepsy Detection in EEG Signal Using Recurrent Neural Network, 53 50, 2019.

Muhammet Varlı has a bachelor's degree in Medical Engineering and Electrical-Electronics Engineering from Karabuk University. He holds a master's degree in Biomedical Engineering and is currently pursuing a Ph.D. in Electrical and Electronics Engineering. Research interests; includes signal processing, image processing, machine learning, deep learning.

Hakan Yılmaz has a Ph.D. in computer engineering and continues his academic activities in the medical engineering department. His main areas of study are medical image processing, machine learning and programming languages.